

Phase retrieval based on transport of intensity equation and image interpolation

Cheng Hong, Deng Huilong, Shen Chuan, Wang Jincheng, Wei Sui

(Key Laboratory of Intelligent Computing & Signal Processing, Ministry of Education, Anhui University, Hefei 230039, China)

Abstract: Phase, as an important property of light field, is difficult to be obtained by the existing detection equipment, which can only detect the intensity information of the light field, however, losing the phase information, hence the "phase problem" can be summarized as the demand of retrieving a sample's complex-field from measurements of intensity. Transport of intensity equation (TIE) based method is one of the typical phase retrieval approaches. When the intensity distribution of the test plane and the axial intensity derivative are known, the phase distribution of the test plane can be calculated directly by solving the equation. Conventionally, intensity derivative is approximated by a finite difference between one in-focus image and one defocused image or two defocused images recorded symmetrically about the focal plane, therefore the proper selection of the distance parameter between defocused image and in-focus image becomes particularly important. A novel approach combining the image interpolation and lens-based TIE was proposed. Firstly, the relationship among two defocused images and one focused image captured was described in geometrical optics model. Secondly, new defocused images with different blur parameters were calculated by image interpolation. Lastly, these new images interpolated and the focused images captured were applied to calculate the phase information. The method could obtain the desired intensity distribution at any positions rapidly with only three captured intensity images, without the mechanical movement of CCD or sample, providing an available way for some special occasions that the intensity acquisitions at appropriate location existed a certain restriction. A practical image acquisition platform was also constructed, the interpolated intensity image was compared with the intensity image obtained by CCD to verify the correctness of the interpolation result, the phase retrieval results under two different computational intensity derivative conditions were given relatively. The experimental results presented verified the feasibility and effectiveness of the method.

Key words: geometric optics; phase retrieval; transport of intensity equation; image interpolation; optical processing;

CLC number: O435 **Document code:** A **DOI:** 10.3788/IRLA201847.1026003

光强传输方程与图像插值融合的相位恢复

程 鸿, 邓会龙, 沈 川, 王金成, 韦 穗

(安徽大学 计算智能与信号处理教育部重点实验室, 安徽 合肥 230039)

收稿日期: 2018-05-05; 修订日期: 2018-06-14

基金项目: 国家自然科学基金(61301296, 61377006, 61501001, 61605002);

安徽省高等学校自然科学研究项目(KJ2017A005, KJ2016A029, KJ2015A114); 安徽省自然科学基金(1608085QF161)

作者简介: 程鸿(1981-), 女, 副教授, 博士, 主要从事计算信号处理方面的研究。Email: chenghong@ahu.edu.cn

摘要: 光强传输方程作为典型的相位恢复技术,在已知待测面光强分布与光强轴向微分时,可以通过求解该方程直接得到待测面的相位分布。强度微分可以通过采集沿传播方向的不同散焦面的光强信息以计算强度差分来估计,由此,散焦面的适当选择变得尤为重要。将光强传输方程与图像插值法相结合,在几何光学模型下描述采集的散焦面光强分布与聚焦面光强分布之间的关系,再利用图像插值法计算出模糊参数不同的散焦面的光强分布,由新得到的散焦图和采集的聚焦图代入光强传输方程以计算出相位。该方法只需要采集三幅强度图像,即可计算获得其他位置的强度图像,避免了采集设备的多次移动,也为某些特殊情况下无法获取适合位置的强度图像提供了一种解决途径。实验中搭建了一个实际的光强图像获取系统,所得结果验证了所提算法的有效性。

关键词: 几何光学; 相位恢复; 光强传输方程; 图像插值; 光学处理

0 Introduction

When a wave interacts with a sample, details of the sample are imprinted on the wave's three properties: intensity, wavelength and phase. Intensity and wavelength are familiar as brightness and color, phase is an inherent characteristic important component bearing the information of the refractive index or the optical thickness. Unfortunately, the frequency of light propagation in space is about 3.1×10^{15} rad/s. No equipment can have such a response speed to catch the phase directly^[1].

The goal of phase retrieval is to extract the phase from intensity measurements. A popular method for phase retrieval is based on the transport-of-intensity equation (TIE), which was introduced by Teague^[2]. TIE-based phase retrieval has been increasingly investigated during recent years due to its unique advantages: it is non-interferometric, computationally simple, no need to phase unwrapping, and does not require a complicated optical system^[3-4]. Also, it overcomes the limitations of iterative methods such as iterative uncertainty and slow convergence.

TIE establishes the quantitative relationship between the longitudinal intensity variation (that is, intensity derivative) and phase using a second-order elliptic partial differential equation. Conventionally, intensity derivative is approximated by a finite difference between one in-focus image and one defocused image or two defocused images recorded

symmetrically about the focal plane^[5]. It should be noted that the distance parameter between defocused image and in-focus image (defocus step) have some restrictions. That is to say, if the defocused images used with too large defocus step to compute the intensity derivative, it will result in a higher error. Besides, many applications have also mentioned the importance of choosing the appropriate defocus distance^[6-8]. How to use the images recorded to calculate the image at appropriate location and then solve the TIE is an important issue should to be addressed.

The purpose of view interpolation is to analyze the two (or more) images captured by the rigid body motion of the camera so as to obtain images under the new viewpoint. At present, the traditional view interpolation algorithm is mainly based on graphics and image methods. The former is abnormally difficult to model with extremely slow drawing speed, and the realism of the image is not guaranteed. Although the latter can interpolate new views located at different viewpoints by appropriately transforming through a previously acquired sequence of images, but meanwhile intensive matching algorithms need to be used, however matching now is still a bottleneck problem in computer vision.

It is known that when the camera focuses, the captured image is clear; when the camera is defocused, the captured image is blurred. The degree of blurring at different points on the image varies with the depth of the object in the scene. The image

information of the new position can be estimated by using the fuzzy information of the image. The TIE-based phase recovery algorithm itself requires focusing and defocusing images. Therefore, a novel image approach for phase retrieval based on defocused image interpolation is proposed in this paper. Firstly, the relationship among two defocused images and one in-focus image is described in geometrical optics model. Secondly, a new desired defocused image at appropriate location is calculated by image interpolation. Lastly, this new image interpolated and images recorded are applied to calculate the TIE and retrieve more accurate phase information. This method avoids the matching problem of correspondence points in stereo vision and motion vision.

1 Transport of intensity equation

In a natural scene, it is generally necessary to use a lens for imaging. A wave propagation model with lens is given as shown in Fig.1. The input object is placed in front of the lens. The distance between the object and lens is d . The focal length of lens is f . The lens-based TIE is described in Ref.[9]:

$$-\nabla \cdot (I_v \nabla \varphi_v) \cong \frac{2\pi}{\lambda} \frac{\partial I}{\partial z} \quad (1)$$

where $\varphi_v(x,z)$ and $I_v(x,z)$ are phase and intensity in the focal plane respectively. This equation can be solved by Fourier method^[10].

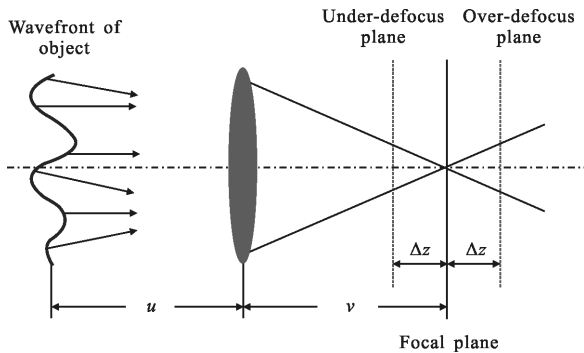


Fig.1 Wave propagation model with lens

In order to reduce the error of intensity derivative, $\partial I(x,z)/\partial z$ can be taken advantage of finite

difference approximation of two defocused intensity images in the positions of $z_0+\Delta z$ and $z_0-\Delta z$,

$$I(x,z+\Delta z)-I(x,z_0-\Delta z)=\frac{\partial I(x,z_0)}{\partial z}(2\Delta z)+O(\Delta z^2) \quad (2)$$

here $I(x,z+\Delta z)$ and $I(x,z_0-\Delta z)$ represent defocused images^[11]. At the same time the error is reduced to second order $O(\Delta z^2)$. Although the above theory is derived in coherence, A. V. Martina et al^[12] proposed that if we choose the central defocus plane at $z=0$, then the incoherent contributions can be removed, provided that a good estimate for the intensity derivative can still be obtained with the additional constraint implied by spatial incoherence, the standard TIE can be used in the $z=0$ plane even with spatial incoherence present.

The phase information $\varphi_v(x,z)$ in the focal plane can be obtained by solving Eq. (1). The intensity information $I_v(x,z)$ can be measured by experiment directly, thus $U_v(x,y)$ is calculated using $U_v(x,y)=\sqrt{I_v(x,y)} \exp[i\varphi_v(x,y)]$. According to the reversibility of light path, the complex amplitude $U_0(x,y)$ of object plane can be acquired. One should pay more attention that function $U_0(x,y)$ has the similar form as $U_v(x,y)$.

$$U_0(x,y)=\sqrt{I_0(x,y)} \exp[i\varphi_0(x,y)] \quad (3)$$

thus the phase distribution $\varphi_0(x,y)$ can be obtained.

In practical calculation, the defocus step Δz is an important parameter which needs to consider seriously. On the one hand, Δz should be as small as possible to make the approximation effective. On the other hand, Δz should be the focused Rayleigh depth at least, so the difference between $I(x,z+\Delta z)$ and $I(x,z_0-\Delta z)$ can be revealed^[13-14]. That is to say, if the defocused images with too large defocus step are used to compute the intensity derivative, it will result in a higher error. How to use images recorded to calculate the desired image at appropriate location will be discussed in the follow section.

Where Δz is some finite defocus distance, the upper limit of this parameter is determined by the highest spatial frequency f_{max} of the object, which can be expressed as $\Delta z < 1/\pi \lambda f_{max}^2$, the noise during the

intensity measurement determines the lower limit of Δz , which can be expressed as $\Delta z > k\sigma/\sqrt{2} I \nabla^2 \varphi$ (assume that the noise is Gaussian noise with standard deviation σ).

2 Lens-based TIE on image interpolation algorithm

2.1 Algorithm principle

We consider the image formation process in a real aperture camera with employing a thin lens. When a point light source is in focus, all light rays that are radiated from the object point and intercepted by the lens converge at a point on the image plane. Following geometric optics shown in Fig.2, when the point is in focus, we can derive the following equation:

$$\frac{1}{u} + \frac{1}{v} = \frac{1}{f} \quad (4)$$

where u is the distance of lens-to-object plane, f is the focal length of the lens, v is the distance of lens-to-focal image plane.

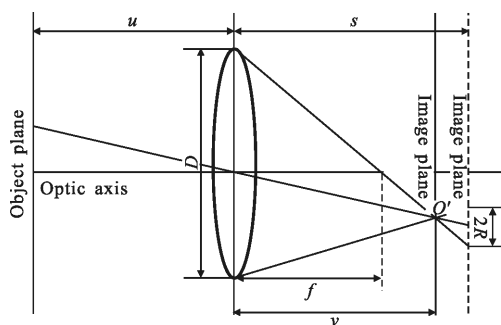


Fig.2 Defocused optical system model

When the point is not in focus, its image on the image plane is no longer a point but a circular patch of radius R that defines the amount of defocus associated with the depth of the point in the scene. It can be shown that

$$\sigma = \frac{kD(s-v)}{2v} \quad (5)$$

where σ is the blur parameter, s is the distance of lens-to-defocus image plane, D is the aperture diameter. The ratio coefficient k is a constant.

Assuming a diffraction-limited lens system and a

constant depth in the scene, the point spread function (PSF) of the camera system at a point (x, z) may be approximately modeled as a circularly symmetric 2-D Gaussian function^[15].

$$h(x, z) = \frac{1}{2\pi\sigma^2} \exp\left(-\frac{x^2 + y^2}{2\sigma^2}\right) \quad (6)$$

Let $I_v(x, z)$ be the focus image of the scene. The observed defocused image $I(x, z)$ is given by

$$I(x, z) = I_v(x, z) * h(x, z) \quad (7)$$

It is assumed that the two defocused image images $I_1(x, z)$ and $I_2(x, z)$ have been obtained, and the blur parameters are σ_1 and σ_2 respectively. The new defocused image can be calculated by the interpolation method. First of all, we construct a warp function to determine the pixel location of the interpolation image.

$$W(U_1, \alpha) = \alpha U_1 + (1-\alpha)U_2 \quad (8)$$

where $\alpha \in [0, 1]$. Set $U_1 = (u_1, v_1, z_1)^T \in I_1$ and $U_2 = (u_2, v_2, z_2)^T \in I_2$ are a pair of corresponding points, $U_3 = (u_3, v_3, z_3)^T$ corresponding to the point of the interpolation image, then the form of wrap function is as follows:

$$U_3 = \alpha U_1 + (1-\alpha)U_2 \quad (9)$$

Corresponding blur parameters are satisfied with

$$\delta_3^2 = \alpha\delta_1^2 + (1-\alpha)\delta_2^2 \quad (10)$$

The known defocused images can be expanded to form a scattered space, then the needful image can be obtained from the known images^[16]:

$$\zeta(I_3) = \zeta(I_v) \exp\left[-\frac{1}{2}[\alpha\sigma_1^2 + (1-\alpha)\sigma_2^2](\omega_x^2 + \omega_y^2)\right] = \{\zeta(I_1)\}^\alpha \times \{\zeta(I_2)\}^{1-\alpha} \quad (11)$$

where ζ denotes the Fourier transform.

Details of our proposed phase retrieval method in the lens-based TIE on image interpolation algorithm are summarized as follows.

2.1.1 TIE based image interpolation

Input: three images including one focused image $I_v(x, y)$ and two defocused images $I_1(x, y)$ and $I_2(x, y)$.

(1) Calculate the blur parameter σ by solving Eq.(5);

(2) Construct α using Eq.(10);

(3) Obtain the new intensity image $I_3(x, y)$ by

solving Eq.(11);

(4) Calculate $\varphi_0(x,y,z)$ using Fourier method;

(5) Correct the phase aberration with phase mask $\varphi(m,n)$;

(6) Calculate $U_0(x,y)$ according to the reversibility of light path;

(7) Obtain $\varphi_0(x,y,z)$ by solving Eq.(3).

Output: phase distribution $\varphi_0(x,y)$ at object plane.

2.2 Experiments

In this letter, we propose a novel phase retrieval technique combined the image interpolation and lens-based TIE. A practical image acquisition platform is also constructed shown in Fig.3. The test sample is installed on the holder. It is illuminated by an expanded collimated laser beam and the illumination beam is linearly polarized. The condensing camera lens is fixed on V-clamp. The focal length of lens can be changed from 70 mm to 210 mm. The CCD with 1 388 pixel \times 1 040 pixel is fixed on a high-precision translation stage and then move with this stage back and forth. The resolution of translation stage is 0.001 mm. In addition, the moving distance can be read accurately on the translation stage panel. We use this image acquisition platform to record intensity images and defocus step. In the following experiments, we will compare the interpolated images with the photographed images, and the correctness of interpolation results is analyzed by the results of phase retrieval.

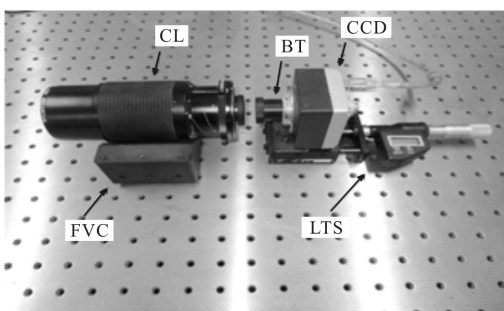


Fig.3 Image acquisition optical system platform

The first group of real experiments test the effectiveness of the image interpolation method. The

parameters are set as follows: the focal length of lens $f=70$ mm, the radius of the aperture $D=50$ mm, lens-to-object plane distance $u=430$ mm. Intensity images at positions $z=0$, $z=0.2$ mm and $z=0.8$ mm are shown in Fig.4(a)–(c). The values of the interpolation coefficients corresponding to $z=0.3$, 0.4, 0.5, 0.6, 0.7 mm are shown in Tab.1 depending on the position of the interpolation. The interpolated defocused image at the different planes are shown in Fig.4 (d)–(h). It can be seen that this method can obtain the intensity images at different positions more accurately.

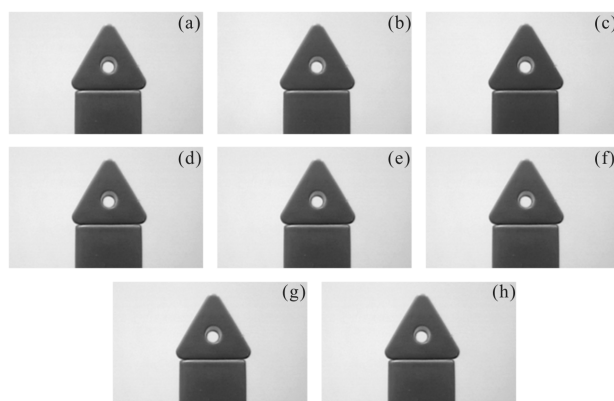


Fig.4 Captured images used optical system platform: (a) $z=0$, (b) $z=0.2$ mm, (c) $z=0.8$ mm and calculated results, (d)–(h) interpolated image at $z=0.3, 0.4, 0.5, 0.6, 0.7$ mm

Tab.1 Interpolation coefficients at different positions

z/mm	0.3	0.4	0.5	0.6	0.7
α	0.084 2	0.201 8	0.352 3	0.535 7	0.751 7

In the second group of experiments, we select two cube boxes with physical size 11 mm \times 11 mm \times 11 mm as experimental subjects. The distance between two objects is 32 mm. Other parameters are set as follows: the focal length of lens $f=70$ mm, the radius of the aperture $D=50$ mm, lens-to-object plane distance $u=430$ mm. Intensity images at positions $z=0$, $f=0.2$ mm and $z=0.4$ mm are shown in Fig.5 (a) –(c). The interpolated defocused image at the position $z=0.3$ mm is shown in Fig.5 (d). Phase result obtained according to the experimental procedure described above is presented in Fig.5(e). As expected, the closer the object to the camera, the darker it appears on the retrieved

phase image. Of course, the gray scale of the depth is relative.

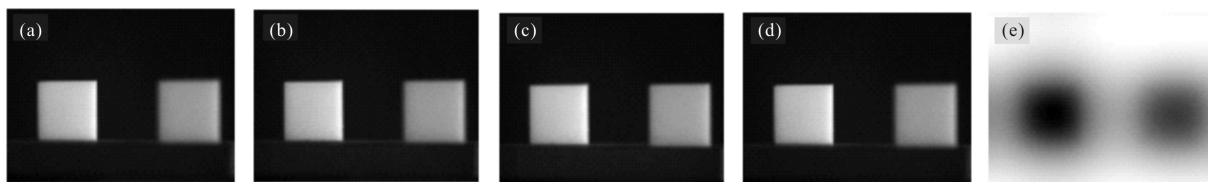


Fig.5 Captured images used optical system platform: (a) $z=0$, (b) $z=0.2$ mm, (c) $z=0.4$ mm and calculated results, (d) interpolated image at $z=0.3$ mm, (e) retrieved phase

In order to verify the correctness of the interpolation result, the interpolated intensity image and intensity image obtained by CCD at $z=0.3$ mm are defined as I_i and I_o respectively. The relative mean square deviation (root-mean-square, RMS) is defined as follows:

$$RMS=100 \cdot \sqrt{\frac{\sum (I_i - I_o)^2}{\sum I_o^2}} \quad (12)$$

The RMS of this group experiment is 5.513 7%. Gray scale contrast diagram of the center line corresponding to the original image and the interpolated image is shown in Fig.6. The blue line is the original intensity value and the red point line is the intensity value retrieved by interpolation method. It could be seen from Fig.6 that the interpolation method can get good result.

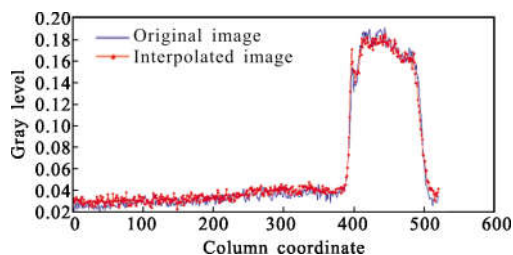


Fig.6 Comparison diagram of gray curve

In the third group of experiments, we firstly interpolated the intensity image at $z=-0.3$ mm as given in Fig.7(d) using three intensity images in Fig.7(a)–(c). The RMS is 4.254 5% compared with the actual image. This time we use Eq.(2) to calculate $\partial I(x,z)/\partial z$ and the phase result is illustrated in Fig.7 (e). The correctness of the interpolated intensity image is reverse proved by the correctness of the phase experimental results. The results of the first group

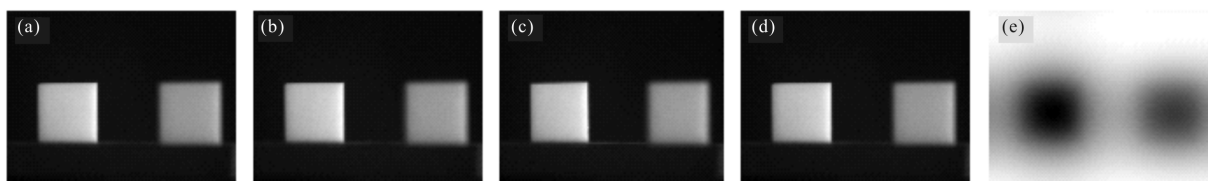


Fig.7 Captured images used optical system platform: (a) $z=0$, (b) $z=-0.2$ mm, (c) $z=-0.4$ mm, and calculated results, (d) interpolated image at $z=-0.3$ mm, (e) retrieved phase

experiments and the second one are consistent.

3 Conclusion

In this paper, we proposed a lens-based TIE on the image interpolation algorithm to retrieve phase for wave propagation model with lens in macro-imaging. An image acquisition optical system platform was constructed to capture focus and defocus images, and

measure the distance between defocus images. The theoretical analysis has been extensively verified by experimental results.

References:

- [1] Zeng Wenwen, Zhong Xiaoping, Li Jingzhen. Retrieving phase from single interferogram by interval inversion method [J]. *Infrared and Laser Engineering*, 2014, 43(9): 3151–3156.

- (in Chinese)
- [2] Teague M R. Deterministic phase retrieval: a Green' s function solution[J]. *JOSA*, 1983, 73(11): 1434–1441.
- [3] Zhang Xiaolei, Zhang Xiangchao, Xiao Hong, et al. Speckle removal in phase reconstruction of digital holography for structured surfaces [J]. *Infrared and Laser Engineering*, 2016, 45(7): 0726002. (in Chinese)
- [4] Liu Beibei, Yu Yingjie, Wu Xiaoyao, et al. Applicable conditions of phase retrieval based on transport of intensity equation [J]. *Optics and Precision Engineering*, 2015, 23(10z): 77–84. (in Chinese)
- [5] Zuo C, Chen Q, Yu Y, et al. Transport-of-intensity phase imaging using Savitzky-Golay differentiation filter-theory and applications[J]. *Optics Express*, 2013, 21(5): 5346–5362.
- [6] Soltani P, Darudi A, Nehmetallah G, et al. Accurate testing of aspheric surfaces using the transport of intensity equation by properly selecting the defocusing distance [J]. *Applied Optics*, 2016, 55(35): 10067–10072.
- [7] Zhang X B, Oshima Y. Experimental evaluation of spatial resolution in phase maps retrieved by transport of intensity equation [J]. *Journal of Electron Microscopy*, 2015, 64(6): 395–400.
- [8] Ma C, Lin X, Suo J, et al. Transparent object reconstruction via coded transport of intensity[C]//Proceedings of the IEEE Computer Society Conference on Computer Vision and Pattern Recognition, 2014: 3238–3245.
- [9] Cheng H, Wei S, Zhang W, et al. Phase retrieval in lens-based Fresnel wave propagation model [J]. *Optical Engineering*, 2013, 52(7): 074102.
- [10] Zuo C, Chen Q, Huang L, et al. Phase discrepancy analysis and compensation for fast Fourier transform based solution of the transport of intensity equation [J]. *Optics Express*, 2014, 22(14): 17172–17186.
- [11] Ishizuka K, Allman B. Phase measurement of atomic resolution image using transport of intensity equation [J]. *Journal of Electron Microscopy*, 2005, 54(3): 191–197.
- [12] Martin A V, Chen F R, Hsieh W K, et al. Spatial incoherence in phase retrieval based on focus variation [J]. *Ultramicroscopy*, 2006, 106(10): 914–924.
- [13] Etienne C, Pierre M, Christian D, et al. Simultaneous amplitude-contrast and quantitative phase-contrast microscopy by numerical reconstruction of Fresnel off-axis holograms[J]. *Applied Optics*, 1999, 38(34): 6994–7001.
- [14] Huang S, Xi F, Liu C, et al. Frequency analysis of a wavefront curvature sensor: selection of propagation distance [J]. *Journal of Modern Optics*, 2012, 59(1): 1–7.
- [15] Surya G, Subbarao M. Depth from defocus by changing camera aperture: a spatial domain approach [C]//Proceedings of IEEE Conference on Computer Vision and Pattern Recognition, 1993: 61–67.
- [16] Namboodiri V P, Chaudhuri S. On defocus, diffusion and depth estimation [J]. *Pattern Recognition Letters*, 2007, 28(3): 311–319.